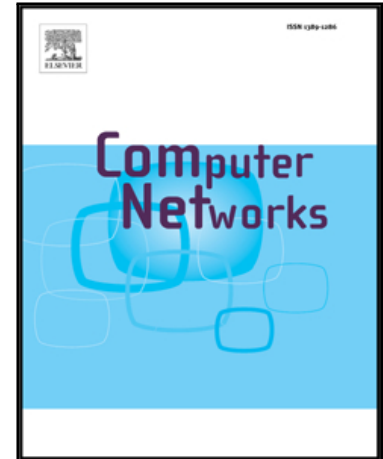


Journal Pre-proof

Skipping-based Handover Algorithm for Video Distribution Over Ultra-Dense VANET

Allan Costa, Lucas Pacheco, Denis Rosário, Leandro Villas, AntonioA.F. Loureiro, Susana Sargento, Eduardo Cerqueira

PII: S1389-1286(20)30218-8
DOI: <https://doi.org/10.1016/j.comnet.2020.107252>
Reference: COMPNW 107252



To appear in: *Computer Networks*

Received date: 17 February 2020
Accepted date: 4 April 2020

Please cite this article as: Allan Costa, Lucas Pacheco, Denis Rosário, Leandro Villas, AntonioA.F. Loureiro, Susana Sargento, Eduardo Cerqueira, Skipping-based Handover Algorithm for Video Distribution Over Ultra-Dense VANET, *Computer Networks* (2020), doi: <https://doi.org/10.1016/j.comnet.2020.107252>

This is a PDF file of an article that has undergone enhancements after acceptance, such as the addition of a cover page and metadata, and formatting for readability, but it is not yet the definitive version of record. This version will undergo additional copyediting, typesetting and review before it is published in its final form, but we are providing this version to give early visibility of the article. Please note that, during the production process, errors may be discovered which could affect the content, and all legal disclaimers that apply to the journal pertain.

© 2020 Published by Elsevier B.V.

Skipping-based Handover Algorithm for Video Distribution Over Ultra-Dense VANET

Allan Costa^a, Lucas Pacheco^{a,*}, Denis Rosário^a, Leandro Villas^b,
Antonio A. F. Loureiro^c, Susana Sargento^d, Eduardo Cerqueira^a

^a*Federal University of Pará (UFPA), Belém, Brazil*

^b*University of Campinas (UNICAMP), Campinas, Brazil*

^c*Federal University of Minas Gerais (UFMG), Belo Horizonte, Brazil*

^d*University of Aveiro, Aveiro, Portugal*

Abstract

Next-generation networks will pave the way for video distribution over vehicular Networks (VANETs), which will be composed of ultra-dense heterogeneous radio networks by considering existing communication infrastructures to achieve higher spectral efficiency and spectrum reuse rates. However, the increased number of cells makes mobility management schemes a challenging task for 5G VANET, since vehicles frequently switch among different networks, leading to unnecessary handovers, higher overhead, and ping-pong effect. In this sense, an inefficient handover algorithm delivers videos with poor Quality of Experience (QoE), caused by frequent and ping-pong handover that leads to high packets/video frames losses. In this article, we introduce a multi-criteria skipping-based handover algorithm for video distribution over ultra-dense 5G VANET, called Skip-HoVe. It considers a skipping mechanism coupled with mobility prediction, Quality of Service (QoS)- and QoE-aware decision, meaning the handovers are made more reliable and less frequently. Simulation results show the efficiency of Skip-HoVe to deliver videos with Mean Opinion Score (MOS) 30% better compared to state-of-the-art algorithms while maintaining a ping-pong rate around 2%.

*Corresponding author

Email addresses: `allan@ufpa.br` (Allan Costa), `lucas.pacheco@itec.ufpa.br` (Lucas Pacheco), `denis@ufpa.br` (Denis Rosário), `leandro@ic.unicamp.br` (Leandro Villas), `loureiro@dcc.ufmg.br` (Antonio A. F. Loureiro), `susana@ua.pt` (Susana Sargento), `cerqueira@ufpa.br` (Eduardo Cerqueira)

Keywords: VANETs, Handover, Mobility Prediction, QoE-aware, and ultra-dense network.

1 1. Introduction

2 Next-generation communications will not only rely on new access tech-
3 nologies, such as Massive MIMO and Millimeter Wave, but they will also
4 take advantage of existing communication infrastructures, such as WiFi and
5 LTE, to provide ubiquitous and efficient communication [1]. In this sense,
6 5G networks will be composed of ultra-dense heterogeneous radio networks
7 compared to 4G systems, increasing the data-rate at the network edge. For
8 instance, densification consists of the massive deployment of macrocells, mi-
9 crocells, small cells, relays, and other communication solutions, achieving
10 both higher spectral efficiency and higher spectrum reuse rates [2, 3, 4].
11 These cells can be used to offload traffic from macrocells to enable the com-
12 munication of all kinds of devices in highly dense, ubiquitous, and hetero-
13 geneous environments, having an immense impact from business and social
14 standpoints [5].

15 The next-generation wireless technology will pave the way for extensive
16 use of high demanding applications such as video-based services for mobile
17 users, anytime and anywhere [6], including real-time distribution of adver-
18 tisement or entertainment videos over vehicular networks (VANETs). One of
19 the critical issues for future and success of video distribution over VANETs
20 will be the ability of heterogeneous networks to support efficient mobility
21 and resource management schemes to increase the Quality of Experience
22 (QoE), while optimizing the usage of high demanded wireless/radio resources
23 [7]. However, the increased number of heterogeneous cells makes mobility
24 management a challenging task for VANETs, since vehicles, especially in ur-
25 ban environments, frequently switch among different heterogeneous networks,
26 *i.e.* vehicles travel leaving an area of a cell to enter another one very often
27 [8]. Many handovers result in excessive signaling overhead, disconnection,
28 and ping-pong effect, *i.e.*, a vehicle disconnects from a cell and afterward
29 connects again to another one moments later [9]. These issues increase the
30 packets/video frames losses, leading to a poor QoE for video applications in
31 such a VANET scenario [10].

32 Skipping unnecessary handovers is beneficial to the network and also to
33 the user's experience [2]. A skipping-based handover consists of avoiding
34 consecutive handovers to maintain the QoE as high as possible, which means

35 reducing the handover frequency by sacrificing some of the best cell con-
36 nectivity associations [11]. Hence, this allows maintaining a longer service
37 duration with the serving cell with at least a minimum service quality level,
38 while reducing signaling overhead and zapping delay. For instance, a han-
39 dover decision based on RSS skips some handovers even if they mean that the
40 user is not receiving the best Signal-to-interference-plus-noise-ratio (SINR) at
41 all times, mitigating ping-pong effect [2]. Skipping-based handover schemes
42 are often associated with mobility prediction information to maximize the
43 connection duration without compromising the network/application perfor-
44 mance [12, 13]. This is achieved by giving priority to cells with the highest
45 probability that the user remains connected for more time [14]. However,
46 skipping-based handover schemes alone are not enough to deliver videos with
47 QoE support. Hence, a handover decision based on a mobility prediction
48 coupled with QoE and Quality of Service (QoS) parameters improve video
49 delivery over VANETs by avoiding ping-pong handovers and by improving
50 the usage of network resources [15].

51 In this article, we propose a multi-criteria skipping-based handover algo-
52 rithm for video distribution over ultra-dense VANETs, called Skip-HoVe. It
53 guarantees seamless handovers in an ultra-dense VANETs scenario to deliver
54 videos with high QoE by taking into account mobility prediction, QoS, QoE,
55 and radio parameters. Skip-HoVe supports an Analytic Hierarchy Process
56 (AHP) to assign different degrees of importance for each criterion. Skip-
57 HoVe considers proactive Ping-Pong avoidance for handover decision, by
58 skipping handovers when QoE and QoS are acceptable and stable. The
59 implementation of Skip-HoVe is available for downloading on Github¹.

60 We tested two mobility prediction technique with Skip-HoVe, namely
61 AutoRegressive Integrated Moving Average (ARIMA) and Kalman Filter
62 (KF). Based on a real-world vehicular dataset analysis, ARIMA provided a
63 higher accuracy for mobility prediction compared with KF. Therefore, we
64 chose ARIMA to be considered as a mobility prediction technique used by
65 Skip-HoVe. Simulation results showed that the Skip-HoVe algorithm deliv-
66 ered videos with QoE 14% better compared to state-of-the-art algorithms in
67 ultra-dense VANET scenarios. For instance, Mean Opinion Score (MOS) re-
68 sults showed a improvement of 30% in subjective evaluations, while ping-pong
69 handover was kept at a low 2% rate. The main contributions of this work

¹<https://github.com/lsidd/hove>

70 are summarized as follows: (i) a skipping-based handover algorithm that
 71 maximizes connection time to a serving cell; (ii) a multi-criteria decision-
 72 making technique for handover decisions in an ultra-dense VANET scenario;
 73 and (iii) simulation results to show the performance of Skip-HoVe to de-
 74 liver videos with QoE support in ultra-dense VANET scenarios compared to
 75 existing handover algorithms.

76 We organize the rest of the article as follows. Section 2 outlines the state-
 77 of-the-art about handover algorithms, their main drawbacks to provide video
 78 dissemination with QoE support. Section 3 describes the Skip-HoVe Al-
 79 gorithm. Section 4 discusses the simulation scenario and results. Finally,
 80 Section 5 presents the conclusion and possible extensions.

81 2. Related Work

82 Gong *et al.* [16] proposed a Fuzzy Analytical Hierarchical Process (FAHP)
 83 algorithm to reduce failure and ping-pong probability in Heterogeneous Ultra-
 84 dense by defining a Time-To-Trigger (TTT) during handover execution. Al-
 85 though it highlights the importance of a multi-parameter handover decision,
 86 the use of TTT can have undesired effects, such as link failures and delayed
 87 handovers [17]. Silva *et al.* [18] proposed an adaptive TTT handover based
 88 on Fuzzy logic and user speed. Such a handover algorithm collects mobility
 89 parameters to predict user location for content dissemination, and not for
 90 handover purposes, showing that offloading from macrocells to Small Cells
 91 can be essential in a heterogeneous environment. One of the main benefits
 92 of the proposed scheme is the reduced ping-pong rates in dense scenarios.
 93 However, it is not intended for multimedia traffic, and, thus, it does not con-
 94 sider QoE for decision making. Liu *et al.* [19] introduced an adaptive TTT to
 95 minimize the impact of frequent handovers in Ultra-Dense Networks. That
 96 work applies a Fuzzy TOPSIS decision to choose the best handover candidate
 97 to achieve proper QoS levels. However, it does not apply predictive metrics
 98 or any QoE monitoring, which can significantly enhance the quality of the
 99 decisions in a VANET scenario.

100 Arshad *et al.* [12] showed that handover introduces an overhead in the
 101 network and is, sometimes, redundant. Skipping some handovers can be
 102 beneficial for the network while maintaining a seamless QoS. However, that
 103 work offers small support for video transmission and may not be suitable for
 104 the strict requirements involved. Demarchou *et al.* [2] studied the challenge of
 105 reducing handover rates (*i.e.*, skipping) in ultra-dense networks. That work

106 considers the trajectory prediction in the skipping decision, but only assumes
 107 a simple model based on position and velocity. Xu *et al.* [20] proposed a
 108 delay oriented cross-tier handover skipping to maximize the performance of
 109 low latency applications in ultra-dense networks. Their work derived an
 110 analytical expression for the adequate capacity of users during the handover
 111 execution and proposed a resource allocation scheme in Target Cells to reduce
 112 blocking probability. It does not employ predictive schemes, or mobility
 113 information into the decision, which may improve the decision quality and
 114 positively impact user QoE.

115 Medeiros *et al.* [21] showed the importance of performing a multi-criteria
 116 handover decision to balance metrics from different layers, namely, radio
 117 measurements, QoS, and QoE. That work uses AHP to balance the metrics
 118 according to predefined importance levels assigned to each, but the algorithm
 119 presents high handover rates, which is harmful to QoE in dense scenarios.
 120 Sargento *et al.* [22] proposed a connection manager for VANETs with hetero-
 121 geneous technologies, VANET Connection Manager (VCM), which is based
 122 on an Analytical Hierarchic Process (AHP) that combines information from
 123 multiple sources (vehicle speed, GPS, heading, RSSI, and available technolo-
 124 gies such as DSRC/WAVE, IEEE 802.11 and 4G Cellular), and decides what
 125 is the best connection available at all times, trying also to minimize the num-
 126 ber of handovers. The AHP is optimized using interaction with a Genetic
 127 Algorithm (GA). This approach includes mobility prediction through the ex-
 128 pected connectivity time but does not include QoE requirements. Zhang *et*
 129 *al.* [23] proposed a classification of applications sensitive and insensitive based
 130 on user experience. A handover decision switches to a more energy-efficient
 131 network during idle timer and a high-performance network when predicted.
 132 Chen *et al.* [24] proposed a QoE estimation to correlate QoS and QoE to
 133 improve user satisfaction, not focusing only on call blocking probability and
 134 handover dropping probability. However, video sharing requires more sub-
 135 jective metrics to describe QoE, such as MOS, which can be mimicked by
 136 machine learning algorithms and integrated into automated decisions.

137 Table 1 summarizes the main characteristics of analyzed handover al-
 138 gorithms in terms of QoE-awareness, mobility prediction-awareness, and
 139 skipping-based handover. Based on our analysis of the state-of-the-art, we
 140 conclude that video distribution over ultra-dense VANETs scenarios requires
 141 an efficient skipping-based handover algorithm to maintain a minimum num-
 142 ber of disruptions and avoid occurrence of ping-pong. Such a scheme requires
 143 efficient mobility prediction technique to improve handover decisions. Fur-

144 furthermore, it is vital to consider a multi-criteria decision scheme to balance
 145 heterogeneous metrics that will directly or indirectly impact user experience
 146 on consuming video services. To the best of our knowledge, Skip-HoVe incor-
 147 porates all of these critical features that have not been provided in a unified
 148 handover algorithm before.

Table 1: Summary of analyzed handover algorithms for ultra-dense VANET scenarios

	Features			Handover Skipping
	Technique Used	QoE-Aware	Mobility Prediction	
Gong et al. [16]	Adaptive TTT			
Silva et al. [18]	Adaptive TTT			
Liu et al. [19]	Fuzzy Logic			
Arshad et al. [25]	Handover Skipping			✓
Demarchou et al. [2]	Handover Skipping		Assumed present	✓
Xu et al. [20]	Delay-Oriented			
Handover Skipping			✓	
Medeiros et al. [21]	AHP	✓		
Sergento et al. [22]	AHP		Expected contact time	✓
Zhang et al. [23]	Q Learning	✓		
Chen et al. [24]	Q Learning	✓		
Skip-HoVe	ARIMA + AHP	✓	✓	✓

149 3. Skip-HoVe Algorithm

150 In this section, we introduce a multi-criteria skipping-based handover
 151 algorithm for video distribution over an ultra-dense VANET scenario, called
 152 Skip-HoVe. It aims to mitigate the adverse effects of frequent handovers
 153 while maintaining an acceptable QoE level of delivered videos. We employ
 154 a proactive skip avoidance condition during a handover decision, as well as
 155 the decision skips handovers when QoE and QoS are acceptable and stable,
 156 while always preferring cells that maximize the connected time.

157 *3.1. Network and System Model*

158 We consider a scenario composed of a set of n vehicles $V = \{v_1, v_2, \dots, v_n\}$
 159 with an individual identity ($i \in [1, n]$). Each vehicle v_i is assumed to have a
 160 radio transceiver to enable the communication between vehicles (V2V) and
 161 with an infrastructure (V2I). For V2I communication, we consider an ultra-
 162 dense cellular network as a K-tier cellular network, where each tier models
 163 the cell of a particular access network, such as macrocells, small cells, or
 164 picocells. In this sense, we consider a set of cells $B = \{b_1, b_2, \dots, b_m\}$ with
 165 an individual identity ($j \in [1, m]$) and deployed in fixed known locations
 166 (x_j, y_j) . The cells across tiers may differ in terms of the spatial density and
 167 transmit power P_j . We also assume a core network with high capacity fibers
 168 connected to avoid congestion on the backhaul links. We denote $N(b_j) \subset B$
 169 as a subset of cells within the radio range (R_{max}) of a given vehicle v_i .

170 Regarding the video content, each compressed video is composed of three
 171 types of frames, *i.e.*, I-, P-, and B-frames [26]. These frames are arranged
 172 into sequences, called a group of pictures (GoP), which contains all the in-
 173 formation required to decode a given video within a period. We denote a
 174 given Video Flow ($VF_i = g_1, g_2, \dots, g_k$) as a set of k GoP g . Each frame in
 175 a given GoP g is divided into one or more video packets (p), depending on
 176 each frame size. Each packet p contains, in addition to the data payload,
 177 other encoder parameters, such as frame-type flag, Id, length, timestamp,
 178 and packet segmentation [26]. To obtain this information, a packet monitor
 179 at the client-side extracts the frame type and intra-frame dependency infor-
 180 mation for each packet p [27], since each VF starts with a sequence header
 181 followed by a GoP header, and then by one or more coded frames.

182 Each vehicle v_i can measure the received signal quality as a radio pa-
 183 rameter from each available cell $N(b_j)$, which can be measured using the
 184 Reference Signal Received Quality (RSRQ). Each vehicle v_i is aware of its
 185 location $L(x_i, y_i, t)$ in a given timestamp t using a positioning system, such as
 186 GPS. Each vehicle v_i travels following a given trajectory $traj_i$ with a speed s_i
 187 ranging between a minimum (*e.g.*, s_{min}) and a maximum (*e.g.*, s_{max}) speed
 188 limit. Each vehicle v_i moves over different areas due to their fast movement,
 189 and, thus, it frequently has a different set of available cells $N(b_j)$.

190 The handover manager entity, such as LTE Mobility Management Entity
 191 (MME), performs all Skip-HoVe handover phases, namely: Measurement,
 192 Decision, and, if a handover is necessary, Execution. This entity must have
 193 a connection to each b_j , such as an S1 interface. Each vehicle v_i communi-
 194 cates with the handover manager logically through its current b_j to report

195 the measurements, which can be requested by the mobility management if
 196 needed. Each vehicle v_i performs measurements, while the MME performs
 197 the handover decision and execution. At the measurement phase, the han-
 198 dover manager must obtain information from both v_i and $N(b_j)$. Afterward,
 199 the handover decision phase considers information collected in the previous
 200 phase to select the b_j that a given vehicle v_i must connect to. Finally, the
 201 handover execution phase is responsible for changing the connection between
 202 a given vehicle v_i from a serving cell to a target cell, chosen by a handover
 203 manager. In the following, we introduce more details about each phase.

204 3.2. Measurement Step

205 Skip-HoVe algorithm collects information from both vehicle v_i and avail-
 206 able cells $N(b_j)$ at the measurement step. Specifically, Skip-HoVe gets from
 207 the vehicle v_i information about its estimated QoE, current location, QoS,
 208 and radio parameters. On the other hand, Skip-HoVe collects QoS and QoE
 209 information from the serving and candidates cells $N(b_j)$ to understand their
 210 performance to make a better decision. The handover manager assigns the
 211 maximum QoS and QoE values as soon as a given cell is idle to give preference
 212 to such cells, and, thus, providing load balancing. In the following, we intro-
 213 duce the description of the mobility prediction, QoE, and QoS monitoring
 214 modules.

215 3.2.1. Mobility Prediction

216 Vehicle mobility is approximately linear, increasing the accuracy of vehic-
 217 ular mobility prediction [28]. In this sense, a mobility prediction algorithm,
 218 such as ARIMA or KF [28], enables to estimate the position $L(x_i, y_i, t + 1)$
 219 of a given vehicle v_i in a future timestamp $t + 1$ based on the vehicles speed
 220 and location using kinematics equations. Based on the mobility prediction,
 221 it is possible to avoid connections to a cell that might no longer be avail-
 222 able in the future. It is useful to treat mobility as a time series, where each
 223 measurement constitutes an entry for the predictor to adjust the prediction
 224 model. The prediction granularity, in a spacial and temporal context, may
 225 be defined by a measurement frequency. For instance, Skip-HoVe performs a
 226 new prediction at every new measurement. We also evaluated the granularity
 227 of mobility prediction ranging from 0.1 to 2 seconds in steps of 0.2 seconds.
 228 Based on our evaluation, we adopted a granularity of 1 second, given the
 229 simplicity of the prediction module, which does not cause significant over-

230 head. However, for other scenarios, this value can be adjusted in order to fit
 231 mobility and computing resources accordingly.

232 Based on the predicted vehicle location, Skip-HoVe computes the distance
 233 $d_{i,j}$ between the vehicle future position $L(x_i, y_i, t + 1)$ and its available cells
 234 $N(b_j)$. Large distance means a cell from which the vehicle is distancing itself,
 235 which should be avoided. However, higher values correspond to a higher score
 236 for such b_j during a handover decision, and, thus, distances vector $Dists$ are
 237 inverted, as shown in Eq. 1.

$$Dists = \left[\frac{1}{d_{i,0}} \quad \frac{1}{d_{i,1}} \quad \frac{1}{d_{i,2}} \quad \dots \quad \frac{1}{d_{i,3}} \right]. \quad (1)$$

238 Several values in the vector $Dists$ could be near zero, due to distances
 239 being too high. In this sense, the vector $Dists$ must be normalized by dividing
 240 every element by the absolute value of the vector $Dists$, which is computed
 241 based on Eq. 2.

$$|Dists| = \sqrt{(d_{i,0})^2 + (d_{i,1})^2 + \dots + (d_{i,2})^2}. \quad (2)$$

242 These values can be fed to the algorithm when computing the score d to
 243 the individual cell b_j , which is computed based on Eq. 3.

$$d = \frac{d_{i,j}}{|Dists|}, \forall d_{i,j} \in Dists. \quad (3)$$

244 3.2.2. QoE-monitor

245 Skip-HoVe considers a low complexity hybrid QoE-monitor running on
 246 a given vehicle v_i to estimate the QoE of a given video flow VF_i , such as
 247 introduced by Medeiros *et al.* [21]. Hybrid QoE video quality assessment
 248 measures the video quality level in real-time based on information from IP
 249 and video codec packet headers [26]. In this sense, a machine learning tech-
 250 nique, namely, a random forest, predicts the MOS value based on frame loss
 251 and video characteristics with low complexity.

252 At the client-side, a packet monitor examines the MPEG bitstream to
 253 verify which frame is lost in a GoP g to compute the frame loss ratio for
 254 each frame type. This is because the loss ratio of each frame and GoP size
 255 differently affect the QoE of transmitted videos [26]. We consider an entire
 256 machine learning process, *i.e.*, training, testing, and validation, to predict
 257 the MOS value for a given video flow VF . In this sense, the QoE-monitor
 258 considers a random forest as a low complexity machine learning technique

259 to correlate the loss rate of I-, P-, and B-frames and GoP size with the
 260 assigned MOS values, achieving a final MOS score. Random forest works
 261 with the concept of forming smaller selections of a tree, informing different
 262 results in these smaller trees, and counting the most chosen solution (*i.e.*,
 263 majority tree) as the answer to a question: what is the estimated MOS value
 264 considering the GoP size and loss ratio of I-, P-, and B-frames?

265 3.2.3. QoS- and signal-monitor

266 Regarding QoS parameters, Skip-HoVe considers PDR to evaluate the
 267 connection between a given vehicle v_i and a cell b_j . Each vehicle v_i computes
 268 the PDR by using packet Ids to detect the lost packets, and associated with a
 269 cell b_j . From the radio perspective, Skip-HoVe algorithm considers the RSRQ
 270 value computed by a given vehicle v_i for each beacon message transmitted
 271 by a cell b_j (both serving and candidate cells). RSRQ measures the received
 272 signal quality in the LTE networks. All measurements are sent to the vehicle's
 273 serving cell and can be requested by the mobility management when they
 274 execute their decision step.

275 3.3. Decision Step

276 At this step, the handover Manager computes a score S_j to each available
 277 cell $N(b_j)$ based on Eq. 4, in order to find the best available cell b_j for a given
 278 vehicle v_i connect to. Skip-HoVe considers multiple metrics with different
 279 priorities for handover decisions, and, thus, it needs to assign a weight w_i for
 280 each input metric M_i , *i.e.*, QoE, QoS, and distance. For instance, weights
 281 can represent how many times QoE is more or less critical than QoS.

$$S_j = \sum_{i=1}^n w_i \times M_i. \quad (4)$$

282 We consider AHP [29] to compute the influence factor for each parameter
 283 since AHP provides a structured technique for decision-making of problems
 284 with multiple parameters involved. AHP decomposes a complex problem
 285 into a hierarchy of simpler sub-problems by combining qualitative and quan-
 286 titative factors for the analysis, allowing the system to find an ideal solution
 287 when there are several criteria considered in the handover process. Specifi-
 288 cally, AHP considers a pairwise comparison between the numerical values of
 289 each collected parameter and its relative degrees of importance, in order to
 290 adjust at runtime its weights. A numeric value represents this pairwise com-
 291 parison, and pairs must not contradict each other, *e.g.*, if a metric i is two

292 times more important than metric j , then j is $1/2$ times as important as i .
 293 We define five importance levels to compare each pair of parameters, which
 294 indicate how vital one parameter is compared to others and the inverted
 295 comparison, as shown in Table 2.

Table 2: Pairwise context importance

$c_{i,j}$	Definition
4	i is much more important than j
2	i is more important than j
1	i is as important as j
$1/2$	i is less important than j
$1/4$	i is much less important than j

296 The handover Manager constructs for each vehicle v_i a comparison matrix
 297 $A = (C_{i,j})_{m \times m}$, where lines and columns represent the metrics to represent
 298 all pair-wise comparisons, as shown in Eq. 5. We denote $c_{i,j}$ as how impor-
 299 tant the i -th element is compared with the j -th element, and m denotes the
 300 number of elements to be compared.

$$A = (C_{i,j})_{n \times n} = \begin{pmatrix} c_{1,1} & c_{1,2} & \cdots & c_{1,n} \\ c_{2,1} & c_{2,2} & \cdots & c_{2,n} \\ \vdots & \vdots & \ddots & \vdots \\ c_{n,1} & c_{n,2} & \cdots & c_{n,n} \end{pmatrix}. \quad (5)$$

301 Matrix $C_{i,j}$ indicates which parameters have higher priority over others,
 302 as shown in Eq. 6. We denote d as the normalized distances computed by Eq.
 303 2, QoE represents the predicted MOS score, and Signal represents the RSRQ
 304 intensity, and QoS means the PDR. For instance, in the first line, we observe
 305 that distance metric d is two times more important than QoE, and four
 306 times more critical than QoS and Signal. It is essential to highlight that if
 307 one criterion is considered to be two times more important than another one,
 308 then the other is $1/2$ as relevant compared with the first, due to the inverted
 309 comparison. Note that the main diagonal of the Matrix must always contain
 310 the value 1, as the metric is compared with itself.

$$C_{i,j} = \begin{matrix} & d & QoE & QoS & Signal \\ \begin{matrix} d \\ QoE \\ QoS \\ Signal \end{matrix} & \begin{pmatrix} 1 & 2 & 4 & 4 \\ 1/2 & 1 & 2 & 2 \\ 1/4 & 1/2 & 1 & 1 \\ 1/4 & 1/2 & 1 & 1 \end{pmatrix} \end{matrix}. \quad (6)$$

311 We find the eigenvector of the matrix ($C_{i,j}$) by dividing each element by
 312 the sum of its column, obtaining the eigenvector $W = [0.5 \ 0.25 \ 0.125 \ 0.125]$,
 313 meaning that that the normalized distances will have a weight of 0.5 for d ,
 314 0.25 for QoE, 0.125 for QoS and 0.125 for Signal as well. We analyzed the
 315 consistency ratio (CR) and the consistency index (CI) of the derived weight
 316 vector, *i.e.*. We analyzed if the derived weight vector is correct. In this sense,
 317 if $CI = 0$ and $CR = CI/RI \leq 0.1$, then the inconsistency of the constructed
 318 comparison matrix is acceptable. Following the process of consistency checks,
 319 we can find out that the comparison matrix ($C_{i,j}$) in Eq. 6 has $CI = 0$ and
 320 $CR = 0$. Therefore, the inconsistency of the constructed pairwise comparison
 321 matrix is acceptable to meet the validation criteria defined for AHP [29].

322 The handover manager performs a product between the eigenvector and
 323 a vector that stores the measured values M_i , obtaining the score of S_i for
 324 all available cells $N(b_j)$. Hence, the handover manager selects the cell with
 325 the highest score S_i , which is the most suitable for the vehicle v_i to connect
 326 at the moment. In the decision/skipping step, the handover manager must
 327 decide if a handover is necessary based on a skipping-based handover decision
 328 since a handover execution is costly and should be avoided if not essential.
 329 Skip-HoVe considers a QoE threshold to trigger the handover, which is de-
 330 fined as 4 for the predicted QoE value [30]. As soon as the predicted QoE
 331 value computed by the QoE-monitor is above this threshold, a handover is
 332 considered unnecessary and skipped, since the video is already delivered to
 333 the vehicle v_i with an acceptable QoE. On the other hand, as soon as the
 334 handover is necessary, the decision step chooses the best available cells $N(b_j)$
 335 for the vehicle v_i to connect, explained hereafter.

336 Skip-HoVe must also analyze if the decision constitutes a ping-pong han-
 337 dover (*i.e.*, when a vehicle leaves a cell and returns within up to 4 seconds
 338 [31]). If so, Skip-HoVe actively skips the execution of the handover, consid-
 339 ered wasteful to network resources. On the other hand, the Skip-HoVe algo-
 340 rithm will consider such a cell for handover decisions after this time window
 341 has passed. Algorithm 1 introduces the primary operations performed by the

342 Skip-HoVe algorithm to deliver video content with QoE support over ultra-
 343 dense VANET. The handover manager executes all three phases, while the
 344 mobile node is connected to any cell.

Algorithm 1: Skip-HoVe algorithm

```

1  $\forall$  vehicles in the network  $v_i \in V$ 
2 while vehicle is connected do
3   Vehicle sends measurements to its serving cell Handover Manager
   to initiate the decision phase
4   for each available cell  $N(b_i) \in B$  do
5     if QoS is above a threshold and not decreasing then
6       Skip handover
7     else
8       Estimate the vehicle's next position
9       Calculate the  $S_i$  score for the cell
10  BestCellId  $\leftarrow$  cell with the highest  $S_i$ 
11  if BestCellId  $\neq$  ServingCellId and BestCellRSRQ  $\geq$  Threshold
   then
12    if Handover is a Ping-Pong then
13      Skip handover
14    else
15      Initiate the handover execution phase

```

345 *3.4. Mobility Prediction Scenario*

346 We consider both ARIMA and KF as use cases for the mobility predic-
 347 tion technique considered by Skip-HoVe, but it can be any other position
 348 prediction scheme. Both ARIMA and KF can be used to predict the vehi-
 349 cle's future position $L(x_i, y_i, t + 1)$ based on the current one $L(x_i, y_i, t)$. In
 350 this sense, Skip-HoVe iterates the mobility prediction algorithm every time a
 351 new measurement arrives, where the intervals between measurements define
 352 the granularity of the filter. In our tests, we adopted the granularity of 1
 353 second.

354 *3.4.1. ARIMA*

355 ARIMA is a statistical model to analyze and forecast time series, which
 356 is one of the most general time series forecasting scheme. ARIMA works by
 357 taking values of series and making them stationary if necessary. A stationary
 358 time series has no trend, and the amplitude of its variations around the mean
 359 is constant. In the ARIMA model, future values of series are assumed to be
 360 a linear combination of past values and past moving averages.

361 ARIMA is described as a 3tuple (p, d, q) , where p corresponds to the
 362 number of past measurements weighted in the estimation, d consists of the
 363 number of differencing series to make statistically stationary, and q corre-
 364 sponds to the number of past moving averages. The basic formulation of the
 365 model is given by Eq. 7. We denote past terms as y , past moving averages
 366 as ϵ , while θ and ϕ are individual weights for each term and will be trained
 367 by the model.

$$y_t = \theta_0 + \phi_1 y_{t-1} + \phi_2 y_{t-2} + \phi_3 y_{t-3} + \dots + \phi_p y_{t-p} + \epsilon_0 + \theta_1 \epsilon_{t-1} + \theta_2 \epsilon_{t-2} + \theta_3 \epsilon_{t-3} + \dots + \theta_q \epsilon_{t-q}. \quad (7)$$

368 The number of past value terms and past moving averages depends on
 369 the studied series, where some series are mostly dependant on weighted past
 370 values and do not need any moving average terms. The model can be repre-
 371 sented by the notation $ARIMA(5, 1, 0)$, which means we use five past terms,
 372 perform one differentiation, and consider no past moving averages.

373 ARIMA is used to forecast a single-variable time series, and, thus, it
 374 has to be done a training step separately for the latitude and longitude
 375 measurements. The first step for the general ARIMA formulation is to define
 376 the differencing order, *i.e.*, the number of times each term is subtracted from
 377 the next one, given by the parameter d , as shown in Eq. 8). The ARIMA
 378 model can be used for the vehicle mobility prediction $L(x_i, y_i, t + 1)$. In this
 379 sense, the model must be trained for each vehicle separately and for each
 380 coordinate (*i.e.*, latitude, and longitude).

$$y_t = \begin{cases} Y_t, & \text{if } d = 0 \\ (Y_t - Y_{t-1}), & \text{if } d = 1 \\ (Y_t - Y_{t-1}) - (Y_{t-1} - Y_{t-2}), & \text{if } d = 2 \\ \text{and so on} & \end{cases} \quad (8)$$

381 *3.4.2. Kalman Filter*

382 KF tries to estimate a state $x_t \in \mathbb{R}^n$ based on previous state x_{t-1} , *i.e.*,
 383 the filter only needs the value of the previous state to estimate the next
 384 one. The state x in a KF is a vector containing a pair of vehicle geographic
 385 coordinates g_t , namely latitude and longitude, at a given moment t (*i.e.*,
 386 $L(x_i, y_i, t)$). Explicitly, we model the process as in a stochastic difference
 387 equation shown in Eq. 9. We denote A as a $n \times n$ matrix that relates the
 388 previous state to the current one, and $w \in \mathbb{R}^n$ as noise estimation.

$$x_t = Ax_{t-1} + w_{t-1}. \quad (9)$$

389 The estimation considers a measurement given by Z_k , as shown in Eq.
 390 10. It can be modeled in terms of the prediction with a correcting factor H
 391 and a noise v_k .

$$Z_k = Hx_k + v_k. \quad (10)$$

392 We define \hat{x}_k^- as previous state, x_k as predicted state, and \hat{x}_k as following
 393 state, where \hat{x}_k^- and \hat{x}_k are real values of the process. We want to estimate x_k
 394 based on the measurement Z_k . The previous and following errors are defined
 395 by e_k^- and e_k , respectively, as shown in Eqs. 11 and 12.

$$e_k^- = x_k - \hat{x}_k^-. \quad (11)$$

$$e_k = x_k - \hat{x}_k. \quad (12)$$

396 Also, the previous state covariance can be defined based on Eq. 13, and
 397 the following state covariance by Eq. 14 as the expected value of the error,
 398 times the error matrix transpose. The goal of the filter is to minimize the
 399 error covariance P_k .

$$P_k^- = E [e_k^- e_k^{-T}]. \quad (13)$$

$$P_k = E [e_k e_k^T]. \quad (14)$$

400 We express the following state as a linear combination of the previous
 401 state, and a correction term proportional to the difference between measure-
 402 ment and state value, as shown in Eq. 15, the value of \hat{x}_k corresponds to the
 403 vector of predicted coordinates in the next measurement g_{t+1} .

$$\hat{x}_k = \hat{x}_k^- + K(z_k - H\hat{x}_k^-). \quad (15)$$

404 The matrix K $n \times m$ is the gain, which should minimize the following
 405 error covariance. We can minimize the error by replacing Eq. 15 into Eq. 12
 406 and, then, deriving the result. In this way, final formulas for computing the
 407 gain of the filter to be used in the estimation is given by Eqs. 16 and 17.

$$K_k = P_k^- H^T (H P_k^- H^T + R)^{-1}. \quad (16)$$

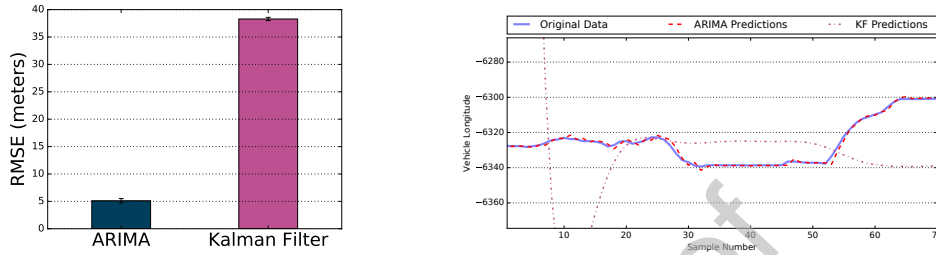
$$K_k = \frac{P_k^- H^T}{H P_k^- H^T + R}. \quad (17)$$

408 3.4.3. Mobility Prediction Accuracy

409 We tested the mobility prediction accuracy of KF and ARIMA in a real-
 410 world vehicular dataset to choose one of them to be part of the handover
 411 algorithm. In this sense, we considered a vehicular mobility trace collected
 412 from approximately 500 taxis from San Francisco [32]. The dataset consists
 413 of GPS measurements of 500+ cabs in the San Francisco bay area over a
 414 period of one month, generating more than 10 million samples. We consider
 415 ARIMA(2,2,1) in such a dataset, *i.e.*, it means that we consider two past
 416 values, the series is differenced twice to make it stationary, and one moving
 417 average term. These parameters were found using a Grid Search estimator
 418 for better performance. We consider 60% of the data for training and the
 419 remaining 40% for tests.

420 Figure 1(a) shows the average Root-Mean-Square Deviation (RMSE) for
 421 the ARIMA and KF to predict each vehicle location in the dataset. By an-
 422 alyzing the results, we can observe that KF has an error 85.7% higher than
 423 the ARIMA. Vehicle movement may be irregular and non-linear for the most
 424 part, but KF is more accurate when the analyzed data has a linear nature
 425 due to its interactive nature. In this sense, KF needs time to adjust to mo-
 426 bility changes in parameters such as speed and direction, *i.e.*, KF makes
 427 adjustments online. On the other hand, ARIMA can predict the mobility
 428 pattern with high accuracy after being trained and is very robust even with
 429 non-linear data. RMSE results can be explained by means of Figure 1(b),
 430 which shows the vehicle's longitude over time for a given vehicle. By analyz-
 431 ing the results, we can conclude that ARIMA predictions are much closer to
 432 the original data points, while KF predictions, in some cases, are very distant

433 from the original data points. For instance, at sample 30, the vehicle turned
 434 (left or right), and ARIMA can predict such vehicle mobility pattern, while
 435 the KF does not detect it.



(a) RMSE for ARIMA and the Kalman Filter Applied in the San Francisco Taxi Dataset

(b) Vehicle Longitude predictions for ARIMA and Kalman Filter applied for one vehicle of San Francisco Taxi Dataset

Figure 1: Mobility prediction results

436 4. Evaluation

437 This section describes the evaluation methodology, including scenario de-
 438 scription, simulation parameters, and metrics used to evaluate the perfor-
 439 mance of different handover algorithms for video distribution in an ultra-
 440 dense VANET scenario.

441 4.1. Scenario description and methodology

442 We implemented the evaluated handover algorithms in the NS-3.29² sim-
 443 ulator and the implementation is available for download on Github¹. NS-3.29
 444 implements the LTE protocol stack for V2I communication. We consider an
 445 ultra-dense VANET scenario such as described by Demarchou *et al.*[2] and
 446 3GPP LTE release 13 [33], considering a $2\text{ km} \times 2\text{ km}$ area with 7 macrocells
 447 covering the whole scenario to some degree, and 100 small cells distributed
 448 through the scenario. Macrocells have a transmission power of 46 dBm, while
 449 small cells have transmission power of 23 dBm. The simulation considers the
 450 Nakagami path loss model, which can be very suitable for urban scenarios
 451 [34]. We conducted 33 simulations with different randomly generated seeds

²<http://www.nsnam.org/>

452 fed to the simulator’s pseudo-random number generator (MRG32k3a). Re-
 453 sults show the values with a confidence interval of 95%. The main simulation
 454 parameters can be seen in Table 3.

Table 3: Simulation parameters

Parameter	Value
Number of vehicles	[50, 100, 150, 200]
Average Speed of Vehicles	43.81 km/h
Number of macrocells	7
Number of Small Cells	100
macrocell Transmission Power	46 dBm
Small Cell Transmission Power	23 dBm
Small Cell Height	10 meters
macrocell Height	45 meters
Propagation Loss Model	Nakagami
Scenario Size	2 km \times 2 km
Video Sequence Tested	Highway [35]
Downlink Frequency	2120 (MHz)
Uplink Frequency	1930 (MHz)

455 We employed the San Francisco cabs mobility trace [32] for the simulation
 456 of traffic and vehicle mobility, as described in Section 3.4.3, varying the
 457 number of vehicles between 50, 100, 150, and 200 to evaluate the scalability.
 458 We consider the real scenario represented by the trace, *i.e.*, the San Francisco
 459 Bay area, due to its direct relation to the real world and human mobility
 460 patterns. Figure 2 depicts the distribution of macrocells and small cells. In
 461 this context, the coverage area of small cells tends to a Voronoi Tessellation
 462 [36], and we assume at least one macrocell is available at all points in the
 463 scenario, as expected in connected vehicles environments. A vehicle traveling
 464 with average speed of 43 km/h crossed the coverage area of 42.8 small cells
 465 during the simulations.

466 We consider a video with moderate complexity (*i.e.*, the Highway video
 467 sequence) levels in terms of motion and spatial complexity, which can be
 468 found in a well-known Video-trace repository [35]. The video has a duration
 469 of 66 seconds encoded with H.264, 30 fps and intermediate size (352 \times 288
 470 pixels), and a bitrate of 210 kbps. It should be noted that all evaluated
 471 videos are streamed in a loop. The decoder uses a Frame-Copy method as

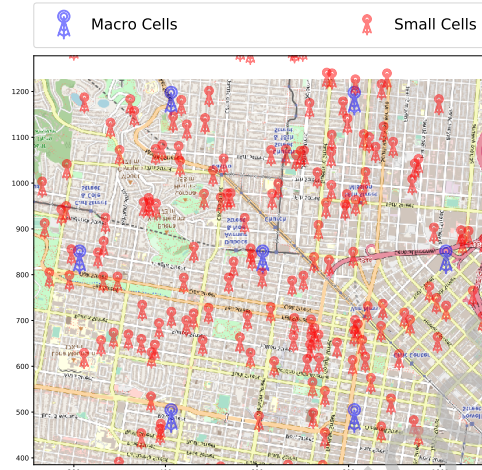


Figure 2: Sample of the simulation scenario with 7 macrocells and several small cells around each macrocell

472 error concealment, replacing each lost frame with the last received one to
 473 reduce the frame loss and to maintain the video quality.

474 We conducted simulations with five different handover algorithms as fol-
 475 lows: (i) *SINR-based handover algorithm* is the most common and traditional.
 476 It considers only the signal strength for handover decision, where a handover
 477 occurs as soon as there is a radio cell with a higher signal strength value
 478 than the current one [37]; (ii) *PBGT handover algorithm*, also known as
 479 Strongest Cell Algorithm, performs a Power Budget based decision, in which
 480 the handover is executed if a neighbor cell has a received strength superior
 481 to the serving cell's plus a hysteresis value, and such difference is main-
 482 tained throughout a previously set Time-To-Trigger [38]; (iii) *NC-Skipping*
 483 *handover algorithm* takes into account the mobility for a Non-Cooperative
 484 Handover Skipping [2]; (iv) *SER handover algorithm* considers QoS and QoE
 485 information for handover decision [21]; and (v) *Skip-HoVe algorithm* consid-
 486 ers multi-criteria for decision making, as well as an enhanced skipping-based
 487 handover algorithm to provide seamless mobility without ping-pong effects
 488 for video distribution, such as described in Section 3.

489 QoE metrics overcome the limitations of QoS metrics for video quality as-
 490 sessment since QoS metrics fail to capture subjective aspects of video content
 491 related to the human experience [15]. In this way, we measured the quality

492 level of each transmitted video using well-known objective and subjective
493 QoE metrics, namely Structural Similarity (SSIM) and MOS, respectively.
494 Specifically, SSIM compares the variance between the original video and the
495 original sequence concerning luminance, contrast, and structural similarity.
496 SSIM values range from 0 to 1, where 0 is the worst case, and 1 means that
497 the transmitted video has the same quality as the original video. We consider
498 the video quality measurement tool (VQMT) to measure the SSIM values of
499 each transmitted video.

500 Subjective evaluation captures all details that might affect the users ex-
501 perience. In this context, MOS is one of the most frequently used metric
502 for subjective evaluation and requires human observers to rating the over-
503 all video quality. For MOS evaluation, we used the single stimulus method
504 of ITU-R BT.500-11 recommendations, since it fits well to a large number
505 of emerging multimedia applications [39]. The human observers watch only
506 once the video and then give a score using ten-grade numerical quality scale,
507 expressing the user experience in words, such as Best (Imperceptible), Good
508 (Perceptible, but not annoying), Fair (Slightly annoying), Poor (Annoying),
509 or Worse (Very annoying). In our subjective evaluation, 31 observers evalu-
510 ated the videos, including undergraduate and postgraduate students, as well
511 as university staff. They had normal vision, and their age ranged from 18
512 to 45 years. The distorted videos were played on a Samsung Galaxy Tab A
513 8.0 with a 8 inches display placed on the back seat of a car headrest, and
514 evaluated by humans to define/score their MOS values during trips between
515 9 AM and 6 PM. The human behavior when they are evaluating videos, the
516 distractions caused by the surrounding environment, and any other (subjec-
517 tive) psychological factors related to the human psychology are out of the
518 scope of this article [40]. For instance, we will not discuss why observers are
519 quick to criticize and slow to forgive or why they take less time to fall when
520 distortions appear than to rise when distortions disappear.

521 We evaluated the handover effectiveness since every handover is a costly
522 process for the infrastructure point-of-view. In this way, a handover should
523 be carefully executed by the handover manager to avoid wasting limited
524 resources. We considered two metrics to evaluate the unnecessary handover
525 decision. The number of handovers is vital to provide details about the
526 average times that a specific handover management algorithm supports a
527 single mobile user to change its cell. Besides, ping-pong is an important
528 metric to evaluate unnecessary handovers, since a ping-pong happens when
529 the handover manager triggers the mobile device to perform a handover to a

530 cell. However, a few moments later (4–6 seconds) the mobile device returns
 531 to the previously connected cell (performing a second handover).

532 4.2. Simulation results

533 Figure 3 shows the objective video quality assessment considering SSIM
 534 values for a video transmitted by different handover algorithms, *i.e.*, Skip-
 535 HoVe, NC-Skipping, SER, SINR-based, and PGBT. By analyzing the results,
 536 we can conclude that videos delivered by Skip-HoVe consistently have a near-
 537 one SSIM value regardless of the number of vehicles, which is not achieved by
 538 the state-of-the-art handover algorithms. For instance, Skip-HoVe delivered
 539 videos with SSIM 28%, 26%, 27%, and 30% higher compared to NC-Skipping,
 540 SER, SINR-based, and PGBT handover algorithms, respectively. This is
 541 because Skip-HoVe provided seamless and reliable handover decisions in an
 542 ultra-dense VANET scenario. To this end, Skip-HoVe considers a skipping
 543 mechanism coupled with mobility prediction, QoS- and QoE-aware decisions,
 544 meaning the handovers are made more reliable and less frequently. In this
 545 sense, Skip-HoVe reduced the I-frame loss rate and the number of handovers,
 546 especially the skip-handover, as discussed in the following. However, other
 547 handover algorithms lack at least one of these characteristics.

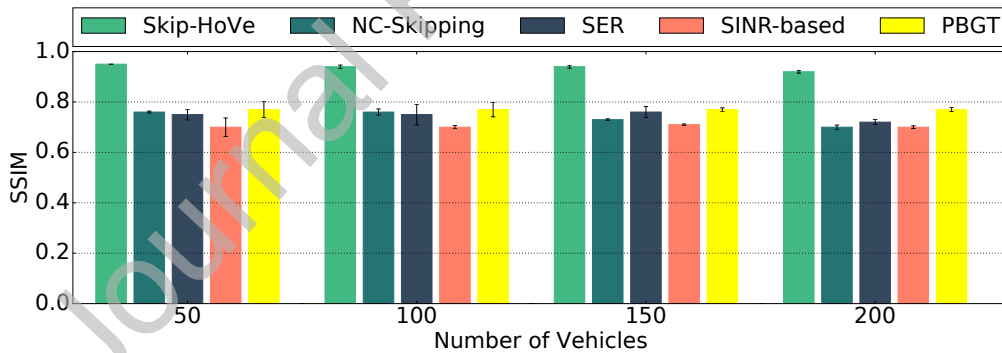


Figure 3: SSIM for videos delivered by different handover algorithms

548 Figure 4 shows the subjective video quality evaluation using the MOS
 549 metric for a video transmitted by different handover algorithms. The set of
 550 transmitted videos used for MOS evaluation is publicly available on YouTube³.

³<http://bit.ly/3aorpoG>

551 By analyzing the MOS results, it is possible to conclude that Skip-HoVe de-
 552 livered real-time videos over VANET scenario with frame losses ranging be-
 553 tween imperceptible to perceptible, but not annoying (*i.e.*, MOS value of
 554 8). At the same time, the other handover algorithms delivered videos with
 555 frame losses between annoying and very annoying (MOS value ranging be-
 556 tween 1 (worse) and 3 (poor)). This is because ultra-dense scenarios lead to
 557 frequent handovers and ping-pong effect, increasing the packet losses, espe-
 558 cially of more important video frames, leading to a poor MOS. In this context,
 559 Skip-HoVe selected a reliable candidate cell for a vehicle to connect to, and,
 560 thus, download the video content considering multiple metrics coupled with
 561 a skipping-based handover decision. On the other hand, NC-Skipping, SER,
 562 SINR-based, and PGBT do not consider efficiently skipping-based handover
 563 decisions coupled with QoE and QoS information. Hence, MOS results show
 564 significant improvements in the quality level of the delivered video using
 565 Skip-HoVe compared to other handover algorithms.

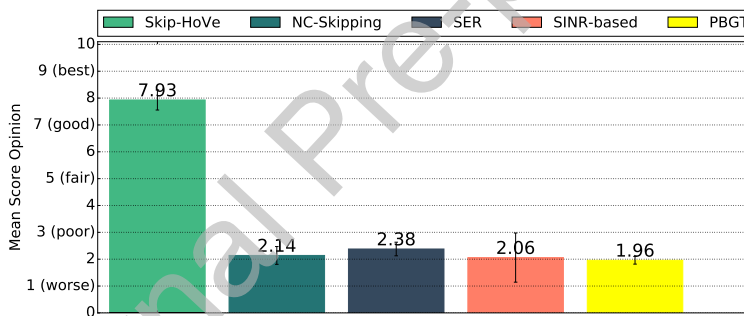


Figure 4: MOS for videos delivered by different handover algorithms

566 Figure 5 shows the I-frame loss ratio of videos delivered via Skip-HoVe,
 567 NC-Skipping, SER, SINR-based, and PGBT handover algorithms, which help
 568 to explain the QoE results. Real-time video dissemination requires low frame
 569 loss, especially of more important video frames, *i.e.*, I-frames, to support
 570 video dissemination with QoE support [15]. The loss of an I-frame causes
 571 severe video distortions based on the user perspective since the video quality
 572 only recovers when the decoder receives an unimpaired I-frame. Based on
 573 the simulation results, we concluded that Skip-HoVe reduced the losses of I-
 574 frames by approximately 94% compared to NC-Skipping, SER, SINR-based,
 575 and PGBT handover algorithms. Hence, Skip-HoVe transmitted priority

576 frames with high deliver probability compared to other evaluated handover
 577 algorithms, increasing the video quality level. On the other hand, state-of-
 578 the-art handover algorithms delivered I-frames with loss ratio ranging from
 579 60% to 80% regardless of the number of vehicles in the scenario, and, thus,
 580 the video takes longer to recover the QoE.

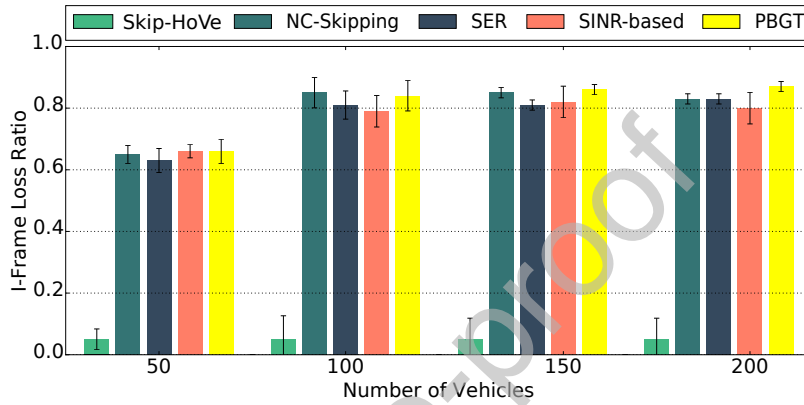


Figure 5: I-Frame loss ratio for videos delivered by different handover algorithms

581 We selected random frames (*e.g.*, frame number 683) from the Highway
 582 video sequence with the highest (Figures 6(b) to 6(f)) and lowest (Figures
 583 6(g) to 6(k)) MOS values for each handover algorithm in order to show the
 584 impact of handover decision executed based on the user perspective, as shown
 585 in Figure 6. Specifically, the frame number 683, from the highway video se-
 586 quence, is a P-frame retrieved by a camera in a car driving in a highway
 587 with a black car on the left highway lane, as shown in Figure 6(a). In both
 588 cases, *i.e.*, video with the highest and lowest MOS values, the frame de-
 589 livered by Skip-HoVe has the same quality compared to the original frame
 590 as can be seen in Figures 6(b) and 6(g), which clearly show the benefits of
 591 Skip-HoVe algorithm for video delivery over ultra-dense VANET scenario.
 592 On the other hand, the frame number 683 captured from the video with the
 593 highest MOS value has few distortions compared to the original frame, which
 594 was transmitted by NC-Skipping, SER, SINR-based, and PGBT handover
 595 algorithms. However, the black on the left highway lane does not appear,
 596 since this frame was lost and it was reconstructed based on the previously
 597 received one. For instance, Skip-HoVe, NC-Skipping, SER, SINR-based, and
 598 PGBT handover algorithms delivered the video with an I-frame loss ratio of
 599 4.48%, 97.03%, 98.51%, 13.43%, and 97.01%, respectively. Finally, for the

600 frame from the video with the lowest MOS value, the frame transmitted by
 601 NC-Skipping, SER, SINR-based, and PGBT handover algorithms are very
 602 impaired compared to the original frame, which makes it impossible to see
 603 anything. This is because this frame was lost, and also many previous ones,
 604 making it impossible to reconstruct the frame based on the previously re-
 605 ceived frames. For instance, the video with the lowest MOS value delivered
 606 by Skip-HoVe, NC-Skipping, SER, SINR-based, and PGBT handover algo-
 607 rithms experienced an I-frame loss ratio of 19.4%, 100%, 100%, 16.19%, and
 608 100%, respectively. Note that even in the best cases, videos usually are not
 609 graded with the best score, this is because the resolution of the original video
 610 is already limited. As mentioned before, the loss of an I-frame causes severe
 611 video distortions based on the user perspective, since QoE only recovers when
 612 the decoder receives an unimpaired I-frame. Since the I-Frames contain the
 613 most amount of information for the image, and given that the videos were
 614 reconstructed using the frame-copy method, algorithms NC-Skipping, SER,
 615 and PGBT only reconstruct the image with the information that changes
 616 from one frame to the other, decreasing QoE. Hence, we can conclude that
 617 Skip-HoVe performs well to deliver videos with the excellent quality com-
 618 pared to state-of-the-art handover algorithms.

619 Figure 7 displays the SSIM of each frame that composes the video se-
 620 quences used in Figure 6 transmitted by the evaluated handover algorithms
 621 and helps to explain the results of Figure 6. When analyzing the results, we
 622 can observe that Skip-HoVe algorithm provided seamless and reliable han-
 623 dover decisions for vehicles to download the video in both cases, *i.e.*, Skip-
 624 HoVe algorithm delivered almost all frames with SSIM close to 1, and all
 625 above 0.8. For the video with the highest MOS value, existing handover algo-
 626 rithms started with a bad connection (*i.e.*, SSIM below 0.7), after some han-
 627 dover decisions, such algorithms increased the SSIM up to 0.9, but the SSIM
 628 reduced afterward. Finally, such handover algorithms delivered the frames
 629 with SSIM raging from 0.3 to 0.7 for the video with the worst MOS value.
 630 This is because state-of-the-art algorithms experience many handovers, es-
 631 pecially ping-pong handovers, which worsen the QoE of delivered videos.
 632 For results of Figure 7(a), Skip-HoVe, NC-Skipping, SER, SINR-based, and
 633 PGBT handover algorithms experienced 25, 7, 35, 25, and 2 handovers, re-
 634 spectively. Out of these handovers, 5, 2, 13, 7, and 0 were considered ping-
 635 pong handovers for Skip-HoVe, NC-Skipping, SER, SINR-based, and PGBT
 636 handover, respectively. Besides, state-of-the-art algorithms do not consider
 637 multiple metrics coupled with a skipping-based handover decision to perform



(a) Original

Frames from video with the highest MOS value:



(b) Skip-HoVe (c) NC-Skipping (d) SER (e) SINR-based (f) PBGT

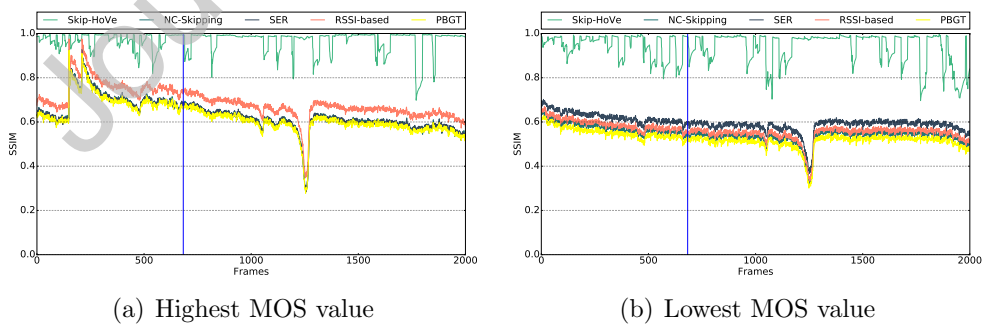
Frames from video with the lowest MOS value:



(g) Skip-HoVe (h) NC-Skipping (i) SER (j) SINR-based (k) PBGT

Figure 6: 683th frame from highway video transmitted via different handover algorithms

638 reliable handover decisions. Hence, we can see that Skip-HoVe is the only al-
 639 gorithm capable of providing a seamless experience, with no QoE drops at all
 640 for the evaluated scenarios, by delivering the essential packets and assuring
 641 high fidelity to the original video sequence.



(a) Highest MOS value

(b) Lowest MOS value

Figure 7: SSIM for all frames that compose the Highway video sequence delivered by different handover algorithms, with the frame depicted in Figure 6 marked in blue

642 Figure 8 shows the number of handovers executed during the simulation
 643 by each handover algorithm. We can see that performing the least amount
 644 of handovers is not necessarily the best approach, as PBGT delivers videos
 645 with poor QoE while performing almost no handovers since it keeps users
 646 connected to the full macrocell in the scenario. On the other hand, the skip-
 647 ping technique employed by NC-Skipping is inefficient in providing acceptable
 648 QoE without a multi-criteria decision. SER has a QoE-aware handover decision,
 649 but it does not consider the skipping-based scheme, accumulating the
 650 negative effect of the high number of handovers. SINR-based, on the other
 651 hand, performs fewer handovers than Skip-HoVe but is highly susceptible to
 652 the occurrence of ping-pong. Interestingly, this causes SINR-based to have
 653 similar results to the ones of SER, showing the significant impact of frequent
 654 handovers even in SER's QoE-based decision. Finally, we can see that even
 655 though NC-Skipping and Skip-HoVe perform roughly the same amount of
 656 handovers, NC-Skipping fails to deliver acceptable QoE and QoS levels.

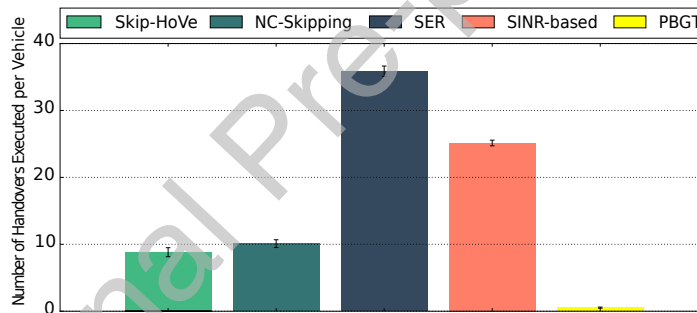


Figure 8: Number of handovers executed by different handover algorithms

657 Figure 9 shows the ping-pong handover rate by Skip-HoVe, NC-Skipping,
 658 SER, SINR-based, and PBGT handover algorithms. It is essential to high-
 659 light that we consider a ping-pong handover as soon as a user leaves a cell
 660 and returns to it within a window of 4 seconds. By analyzing the results,
 661 we can conclude that Skip-HoVe keeps the ping-pong rate around 2%, which
 662 is an indication of a better decision policy that avoids such a phenomenon.
 663 As mentioned before, PBGT performs a smaller amount of handovers, and,
 664 consequently, has a smaller ping-pong probability within the considered win-
 665 dow. On the other hand, NC-Skipping, SER, and SINR-based algorithms
 666 have higher ping-pongs, due to the fact they do not have a transparent bar-
 667 rier against it. Even with a skipping mechanism, these approaches are not

668 coupled with a multiple criteria strategy and are then also susceptible to
 669 ping-pong.

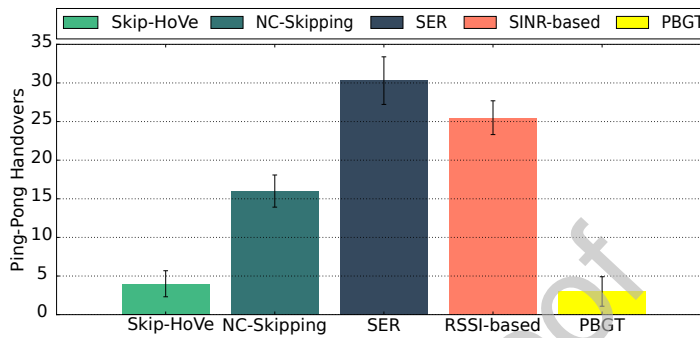


Figure 9: Ping-Pong Handover ratio by different handover algorithms

670 Table 4 summarizes the experimental results obtained for each of han-
 671 dover algorithms for the case of one randomly sampled vehicle. We can
 672 see that in terms of QoE, given in MOS, Skip-HoVe had the highest score
 673 out of all the tested algorithms. Followed by SINR-based, PBGT, SER,
 674 and NC-Skipping, respectively. This happens because Skip-HoVe performs a
 675 QoE-based decision, and also only Skip-HoVe's decision supports the particu-
 676 larities of ultra-dense networks, such as the high number of cells. On average,
 677 Skip-HoVe performed fewer handovers, except the PBGT algorithm, in which
 678 vehicles only left one macrocell for another. Skip-hove, out of the 38 possible
 679 connections, Skip-Hove only made 8 handovers, this is because these han-
 680 dovers were evaluated in order to maintain high QoE, while performing the
 681 fewest possible handovers. NC-Skipping performs almost the same amount
 682 of handovers as Skip-HoVe, but fails to maintain acceptable QoE and QoS.
 683 In the case of SER, the algorithm is very sensitive to fluctuations on QoE,
 684 performing then, a great number of disconnections and ping-pong handovers.
 685 As well as a high I-Frame loss ratio. The SINR-based algorithm, on the other
 686 hand, is very sensitive to random signal fluctuations. Under this algorithm,
 687 when a node is in overlapping coverage areas, handovers are very frequent.
 688 The PBGT algorithm is less sensitive to fluctuations, and generally prefers
 689 macrocells, under this algorithm, the two macrocells that the vehicle crossed
 690 triggered a connection.

Table 4: Results Summary for a Vehicle in the Scenario

Algorithm	MOS	Number of Handovers	Ping-Pong Handovers	I-Frame Loss Ratio	Small Cells Passed	Macrocells Passed
Skip-HoVe	8	8	0	5%	38	2
NC-Skipping	1	10	3	66%	44	1
SER	1	36	21	64%	43	1
SINR-based	2	25	13	67%	43	2
PBGT	2	2	0	67%	39	2

691 Skip-HoVe prevents unnecessary handovers and delivers a seamless experience to end-users.
692

693 5. Conclusion

694 This article introduced a multi-criteria skipping-based handover algorithm for video distribution over ultra-dense VANET scenarios, called Skip-HoVe.
695 Skip-HoVe provides seamless handover decisions, by coupling a handover skipping technique and a multi-criteria handover decision to improve
696 the QoE of video transmissions and reduce the ping-pong rates. In this article, Skip-HoVe considers ARIMA for vehicles mobility prediction, PDR as
697 a QoS criterion, hybrid QoE estimation as the QoE parameter, and RSRQ as the radio parameter. For the handover decision, Skip-HoVe computes the
698 quality level for each cell to select the appropriate cell for the vehicle to connect to by considering AHP to assign different degrees of importance for
699 each criterion. Through these approaches, Skip-HoVe prevents unnecessary handovers and delivers a seamless experience to end-users. Our performance
700 evaluation analysis revealed that Skip-HoVe improved the video delivery up to 14% in SSIM compared to NC-Skipping, SER, SINR-based, and PBGT
701 handover algorithm, and MOS results showed up to 30% better subjective evaluation, while kept the ping-pong rate lower than 2%. For future work,
702 we plan to extend the Skip-HoVe in the following directions: Extend the mobility prediction technique and integrate the handover algorithm for all
703 users on the network, either pedestrians or vehicles; and analyze and correlate the mobility patterns of several users to predict the area congestion and
704 perform efficient offloading of cells and edge services. Finally, another direction is to design integrated solutions where applications can benefit from the
705 Skip-HoVe algorithm and assess their better performance.
706
707
708
709
710
711
712
713
714
715
716

717 **References**

- 718 [1] S. A. A. Shah, E. Ahmed, M. Imran, S. Zeadally, 5G for Vehicular
719 Communications, *IEEE Communications Magazine* 56 (2018) 111–117.
- 720 [2] E. Demarchou, C. Psomas, I. Krikidis, Mobility Management in Ultra-
721 Dense Networks: Handover Skipping Techniques, *IEEE Access* 6 (2018)
722 11921–11930.
- 723 [3] H. Beyranvand, M. Lévesque, M. Maier, J. A. Salehi, C. Verikoukis,
724 D. Tipper, Toward 5g: Fiwi enhanced lte-a hetnets with reliable low-
725 latency fiber backhaul sharing and wifi offloading, *IEEE/ACM Trans-*
726 *actions on Networking* 25 (2017) 690–707.
- 727 [4] H. Ji, S. Park, J. Yeo, Y. Kim, J. Lee, B. Shim, Ultra-reliable and low-
728 latency communications in 5g downlink: Physical layer aspects, *IEEE*
729 *Wireless Communications* 25 (2018) 124–130.
- 730 [5] F. Mohammadnia, C. Vitale, M. Fiore, V. Mancuso, M. A. Marsan,
731 Mobile small cells for adaptive ran densification: Preliminary through-
732 put results, in: *2019 IEEE Wireless Communications and Networking*
733 *Conference (WCNC)*, pp. 1–7.
- 734 [6] J. Nightingale, P. Salva-Garcia, J. M. A. Calero, Q. Wang, 5g-qoe: Qoe
735 modelling for ultra-hd video streaming in 5g networks, *IEEE Transac-*
736 *tions on Broadcasting* 64 (2018) 621–634.
- 737 [7] G. Luo, Q. Yuan, H. Zhou, N. Cheng, Z. Liu, F. Yang, X. S. Shen,
738 Cooperative vehicular content distribution in edge computing assisted
739 5G-VANET, *China Communications* 15 (2018) 1–17.
- 740 [8] E. Ndashimye, S. K. Ray, N. I. Sarkar, J. A. Gutiérrez, Vehicle-to-
741 infrastructure communication over multi-tier heterogeneous networks:
742 A survey, *Computer networks* 112 (2017) 144–166.
- 743 [9] N. Aljeri, A. Boukerche, A two-tier machine learning-based handover
744 management scheme for intelligent vehicular networks, *Ad Hoc Net-*
745 *works* 94 (2019) 101930.

- 746 [10] X. Guan, X. Wan, J.-b. Wang, X. Ma, G. Bai, Mobility aware partition
747 of mec regions in wireless metropolitan area networks, in: IEEE Confer-
748 ence on Computer Communications Workshops (INFOCOM Workshop),
749 IEEE, pp. 1–2.
- 750 [11] R. Arshad, H. ElSawy, S. Sorour, T. Y. Al-Naffouri, M.-S. Alouini, Han-
751 dover management in 5g and beyond: A topology aware skipping ap-
752 proach, *IEEE Access* 4 (2016) 9073–9081.
- 753 [12] R. Arshad, H. ElSawy, S. Sorour, T. Y. Al-Naffouri, M.-S. Alouini,
754 Velocity-aware handover management in two-tier cellular networks,
755 *IEEE Transactions on Wireless Communications* 16 (2017) 1851–1867.
- 756 [13] N. Aljeri, A. Boukerche, Movement prediction models for vehicular
757 networks: an empirical analysis, *Wireless Networks* 25 (2019) 1505–
758 1518.
- 759 [14] A. Mohamed, O. Onireti, S. A. Hoseinitabatabaei, M. Imran, A. Imran,
760 R. Tafazolli, Mobility prediction for handover management in cellular
761 networks with control/data separation, in: 2015 IEEE International
762 Conference on Communications (ICC), IEEE, pp. 3939–3944.
- 763 [15] A. Argyriou, K. Poularakis, G. Iosifidis, L. Tassiulas, Video delivery in
764 dense 5g cellular networks, *IEEE Network* 31 (2017) 28–34.
- 765 [16] F. Gong, Z. Sun, X. Xu, Z. Sun, X. Tang, Cross-tier handover deci-
766 sion optimization with stochastic based analytical results for 5g hetero-
767 geneous ultra-dense networks, in: IEEE International Conference on
768 Communications Workshops, IEEE, pp. 1–6.
- 769 [17] Y. Lee, B. Shin, J. Lim, D. Hong, Effects of time-to-trigger parameter
770 on handover performance in son-based lte systems, in: 2010 16th Asia-
771 Pacific Conference on Communications (APCC), IEEE, pp. 492–496.
- 772 [18] K. D. C. Silva, Z. Becvar, C. R. L. Frances, Adaptive hysteresis margin
773 based on fuzzy logic for handover in mobile networks with dense small
774 cells, *IEEE Access* 6 (2018) 17178–17189.
- 775 [19] Q. Liu, C. F. Kwong, S. Zhang, L. Li, J. Wang, A fuzzy-clustering
776 based approach for madm handover in 5g ultra-dense networks, *Wireless*
777 *Networks* (2019) 1–14.

- 778 [20] X. Xu, X. Tang, Z. Sun, X. Tao, P. Zhang, Delay-Oriented Cross-Tier
779 Handover Optimization in Ultra-Dense Heterogeneous Networks, *IEEE*
780 *Access* 7 (2019) 21769–21776.
- 781 [21] I. Medeiros, L. Pacheco, D. Rosário, C. Both, J. Nobre, E. Cerqueira,
782 L. Granville, Quality of experience and quality of service-aware handover
783 for video transmission in heterogeneous networks, *International Journal*
784 *of Network Management* (2018) e2064.
- 785 [22] S. Sargento, A. Cardote, C. Ameixieira, F. Neves, J. Dias, Method and
786 apparatus for multi-network communication in vehicular networks, *US*
787 *Patent US9439121 B2* (2016).
- 788 [23] D. Zhang, Y. Zhou, X. Lan, Y. Zhang, X. Fu, Aht: Application-based
789 handover triggering for saving energy in cellular networks, in: *2018 15th*
790 *Annual IEEE International Conference on Sensing, Communication, and*
791 *Networking (SECON)*, *IEEE*, pp. 1–9.
- 792 [24] J. Chen, Y. Wang, Y. Li, E. Wang, Qoe-aware intelligent vertical handoff
793 scheme over heterogeneous wireless access networks, *IEEE Access* 6
794 (2018) 38285–38293.
- 795 [25] R. Arshad, H. ElSawy, S. Sorour, T. Y. Al-Naffouri, M.-S. Alouini, Han-
796 dover management in dense cellular networks: A stochastic geometry
797 approach, in: *IEEE international conference on communications (ICC)*,
798 *IEEE*, pp. 1–7.
- 799 [26] J. Greengrass, J. Evans, A. C. Begen, Not All Packets are Equal, Part
800 2: The Impact of Network Packet Loss on Video Quality, *IEEE Internet*
801 *Computing* 13 (2009) 74–82.
- 802 [27] L. Noirie, E. Dotaro, G. Carofiglio, A. Dupas, P. Pecci, D. Popa, G. Post,
803 Semantic networking: Flow-based, traffic-aware, and self-managed net-
804 working, *Bell Labs Technical Journal* 14 (2009) 23–38.
- 805 [28] N. Bui, M. Cesana, S. A. Hosseini, Q. Liao, I. Malanchini, J. Widmer,
806 A Survey of Anticipatory Mobile Networking: Context-Based Classifi-
807 cation, Prediction Methodologies, and Optimization Techniques, *IEEE*
808 *Communications Surveys and Tutorials* 19 (2017) 1790–1821.

- 809 [29] T. L. Saaty, Analytic hierarchy process, *Encyclopedia of Biostatistics* 1
810 (2005).
- 811 [30] E. Liotou, D. Tsolkas, N. Passas, L. Merakos, Quality of experience
812 management in mobile cellular networks: key issues and design chal-
813 lenges, *IEEE Communications Magazine* 53 (2015) 145–153.
- 814 [31] L. Tartarini, M. A. Marotta, E. Cerqueira, J. Rochol, C. B. Both,
815 M. Gerla, P. Bellavista, Software-defined handover decision engine for
816 heterogeneous cloud radio access networks, *Computer Communications*;
817 115 (2018) 21 – 34.
- 818 [32] M. Piorkowski, N. Sarafijanovic-Djukic, M. Grossglauser, CRAW-
819 DAD dataset epfl/mobility (v. 2009-02-24), Downloaded from <https://crawdad.org/epfl/mobility/20090224>, 2009.
820
- 821 [33] E. U. T. R. Access, Study on small cell enhancements for e-utra and
822 e-utranhigher layer aspects (release 12),, 2013.
- 823 [34] L. Rubio, J. Reig, N. Cardona, Evaluation of nakagami fading behaviour
824 based on measurements in urban scenarios, *AEU-International Journal*
825 *of Electronics and Communications* 61 (2007) 135–138.
- 826 [35] Xiph.org video test media [derf’s collection], ????
- 827 [36] F. Baccelli, B. Błaszczyszyn, On a coverage process ranging from the
828 boolean model to the poisson–voronoi tessellation with applications to
829 wireless communications, *Advances in Applied Probability* 33 (2001)
830 293–323.
- 831 [37] J. Kurjenniemi, T. Henttonen, J. Kaikkonen, Suitability of rsrq mea-
832 surement for quality based inter-frequency handover in lte, in: 2008
833 *IEEE International Symposium on Wireless Communication Systems*,
834 *IEEE*, pp. 703–707.
- 835 [38] 3GPP, Evolved universal terrestrial radio access (e-utra); radio resource
836 control (rrc); protocol specification, 3GPP TS 36.331 V9.4.0 (2010-09),
837 *Evolved Universal Terrestrial Radio Access (E-UTRA);Radio Resource*
838 *Control (RRC);Protocol specification(Release 9)* (2011).

- 839 [39] K. Zheng, X. Zhang, Q. Zheng, W. Xiang, L. Hanzo, Quality-of-
840 experience assessment and its application to video services in lte net-
841 works, *IEEE Wireless Communications* 22 (2015) 70–78.
- 842 [40] M. De Felice, E. Cerqueira, A. Melo, M. Gerla, F. Cuomo, A. Baiocchi, A
843 distributed beaconless routing protocol for real-time video dissemination
844 in multimedia vanets, *Computer communications* 58 (2015) 40–52.

Journal Pre-proof



CIÊNCIA E TECNOLOGIA Allan Costa

Allan Costa is a Ph.D. student in Computer Science, working in the area of concentration in Computer Systems, in the line of research in Computer Networks, holds a Master's Degree at UFPA in Computer Science, in the field of Concentration in Computer Systems, working in the line of research in Computer Network. holds a Postgraduate Diploma in Executive MBA in Corporate Finance from Universidade Gama Filho (UGF).



Lucas Pacheco

Lucas Pacheco graduated in Computer Engineering one year in advance, at the Federal University of Pará (2019). Currently pursuing a master's degree in Electrical Engineering at UFPA with a focus on Networks and Distributed Systems. Part of the Smart and Sustainable Cities Laboratory (LaCiS) since 2016, where he develops projects in heterogeneous networks, urban mobility, Network Management, Autonomous Connected Vehicles, and more.



Denis Rosário

Denis Rosário graduated in Computer Engineering from Instituto de Estudos Superiores da Amazônia (2007). In 2010, he obtained a master's degree in Automation and Systems Engineering from the Federal University of Santa Catarina (UFSC), with a sandwich at the CISTER Research Unit of the Instituto Superior de Engenharia do Porto in Portugal (2009). In 2014, he obtained the title of Ph.D. in Co-Tutorship in Electrical Engineering from the Federal University of Pará (UFPA) and in Computer Science from the University of Bern.



Leandro Villas

Leandro Villas has been a professor at the Institute of Computing at UNICAMP since 2013. In 2012 he received the title of Doctor of Computer Science at the Federal University of Minas Gerais, having worked in the area of data collection in wireless sensor networks. He spent a year in the PARADISE laboratory at SITE (School of Information Technology and Engineering) at the University of Ottawa, Canada, as part of his sandwich doctorate. In 2007 he received the title of Master in Computer Science from the Federal University of São Carlos, having worked in the area of routing solutions for wireless sensor networks.



Antonio Loureiro

Antonio Loureiro holds a degree in Computer Science from the Federal University of Minas Gerais (1983), a master's degree in Computer Science from the Federal University of Minas Gerais (1987), and a doctorate in Computer Science from the University of British Columbia, Canada (1995). He is currently a Full Professor at the Department of Computer Science at the Federal University of Minas Gerais.



Susana Sargento

Susana Sargento is a Full Professor at the University of Aveiro and a senior researcher in the Institute of Telecommunications, where I am leading the

Network Architectures and Protocols (NAP) group. Received her PhD in 2003 in Electrical Engineering at the University of Aveiro (with a seven months stay at Rice University in 2000 and 2001). Joined the Department of Computer Science of the University of Porto between 2002 and 2004, and was a Guest Faculty of the Department of Electrical and Computer Engineering from Carnegie Mellon University, USA, in August 2008, where performed Faculty Exchange in 2010/2011.



Eduardo Cerqueira

Eduardo Cerqueira Graduated in Data Processing Technologist at the University of the Amazon (2000), Master in Computer Science at the Federal University of Santa Catarina (2003), Ph.D. in Computer Engineering at the University of Coimbra (2008) and postdoctoral in Computer Engineering at University of Coimbra (2009) and in Computer Science from the University of California at Los Angeles.

Allan Costa; Writing – review & editing

Lucas Pacheco; Formal analysis, Investigation; Methodology, Validation, Visualization, Writing – original draft, Writing – review & editing;

Denis Rosário; Funding acquisition; Investigation; Methodology; Project administration; Resources; Writing – review & editing;

Leandro Villas; Funding acquisition; Investigation; Methodology; Project administration; Resources; Writing – review & editing;

Antônio Loureiro; Funding acquisition; Investigation; Methodology; Project administration; Resources; Writing – review & editing;

Susana Sargento; Funding acquisition; Investigation; Methodology; Project administration; Resources; Writing – review & editing;

Eduardo Cerqueira; Funding acquisition; Investigation; Methodology; Project administration; Resources; Writing – review & editing;

Journal Pre-proof

Declaration of interests

The authors declare that they have no known competing financial interests or personal relationships that could have appeared to influence the work reported in this paper.

The authors declare the following financial interests/personal relationships which may be considered as potential competing interests:

The authors declare that they have no known competing financial interests or personal relationships that could have appeared to influence the work reported in this paper.

Journal Pre-proof